XL CILAMCE
IBERO-LATIN AMERICAN CONGRESS ON COMPUTATIONAL METHODS IN ENGINEERING
NOVEMBER 11-14, 2019
Praiamar Natal Hotel & Convention
Natal, RN-BRAZIL

LATTICE BOLTZMANN SIMULATION OF A 2D BACKWARD FACING STEP AT LOW TO MODERATE REYNOLDS NUMBER: A COMPARISON OF THE STABILITY OF BGK AND TRT COLLISION OPERATORS

Juan P. L. C. Salazar
Luis O. E. dos Santos
Alejandra C. Lago
Diogo N. Siebert
juan.salazar@ufsc.br
luis.emerich@ufsc.br
cas_ale14@hotmail.com
diogo.siebert@ufsc.br
Universidade Federal de Santa Catarina
Rua Dona Francisca 8300 - Bloco U, 89.219-600, Joinville-Santa Catarina, Brazil
Luiz A. Hegele Jr.
luiz.hegele@udesc.br
Universidade do Estado de Santa Catarina
Avenida Lourival Cesário, s/n, Edifício Alcides Abreu, 88.336-275, Balneário Camboriú-Santa Catarina, Brazil

Abstract. In this study we present Lattice-Boltzmann simulations of a 2D backward facing step flow in the low to moderate Reynolds number range. A single relaxation time model for the collision operator (BGK) is compared to a two-relaxation-time model (TRT) and 3-D experiments of [Tihon, J., Penkakova, V. and Pantzali, M., 2010. The effect of inlet pulsations on the backward- facing step flow. European Journal of Mechanics B-Fluid, Vol. 29, pp. 224-235]. Special attention is devoted to detachment and reattachment locations along the line of center of the computational domain, and to numerical stability comparison between BGK and TRT as a function of grid resolution for similar accuracy. A traditional finite volume method is also implemented for comparison. Results show that the BGK implementation achieves similar accuracy at lower grid resolution, maintaining numerical stability of the method at reduced computational cost. BGK and TRT implementations agree with experiments and the finite volume method at Reynolds number of 590.

Keywords: backward-facing step, Lattice-Boltzmann Method, stability, two-relaxation time operator, Bhatnagar-Gross-Krook operator

1 Introduction

The backward-facing step flow (BFS) is a canonical problem in fluid mechanics. A scheme of the flow is shown in Fig. 2. It consists of a rectangular channel of width W where the flow enters through the channel inlet (I), followed by a constant area section of length l_u and height H after which a step of height h is introduced, giving rise to an abrupt expansion. The flow then proceeds to the outlet (II) through a constant area section of length l_d, height $H + h$ and width W. Depending on the Reynolds number $Re_h = Uh/\nu$, where U is the inlet mean velocity and ν is the kinematic viscosity of the fluid, the flow will exhibit very different behavior. Unless the $Re_h \sim \mathcal{O}(1)$, there will be flow separation at the step. Other important parameters in this problem are the expansion ratio $ER = 1 + h/H$ and the aspect ratio $AR = W/h$. In spite of the simple geometry, a complex array of phenomena can be investigated, including flow instability, laminar to turbulence transition, boundary layer separation, shear layer reattachment, recirculation, etc. [1, 2].

Often BFS is a demanding test bench for turbulence models [3–5]. There is extensive experimental [6–9] and numerical work on this subject, including full three-dimensional numerical solutions of the Navier-Stokes equations covering a wide range of Reynolds numbers, from laminar to turbulent [10–13].

Over the last couple of decades, simulation methods based on gas-kinetic theory have developed significantly, in particular the so called Lattice-Boltzmann Method (LBM) [14] has proven itself in applications such as turbulence, multiphase flow and microfluidics [15]. In previous work [16] we validated a LBM code with a simulation of a 2-D BFS with $ER = 2$ at two Reynolds numbers, $Re_h = 124$ and $Re_h = 590$, and compared the results to experiments and simulations reported in Tihon et al. [17]. In this paper we are interested in investigating the numerical stability of two widely used collision operators, the Bhatnagar-Gross-Krook (BGK) [18] and the two-relaxation-time (TRT) [19] operators. In §2 we present an overview of LBM and describe simulation specifics. This is followed by results and discussion in §3. Finally, we provide conclusions and a general outlook for future work in §4.

2 Numerical methods

2.1 The Lattice-Boltzmann Method

The Lattice-Boltzmann method (LBM) is a numerical method for the simulation of fluids, based on the Kinectic Theory of Gases. The LBM is built on the mesoscopic scale, in which the system description is done using a single particle distribution function, $f_i(\mathbf{x}, t)$, representing the number of particles with velocity $\mathbf{c}_i$ at the site $\mathbf{x}$ and time t. The physical and velocity space are discretized, therefore the particles are restricted to a discrete lattice, in such a manner that each group of particles are allowed to move only in a finite number of directions and with a limited number of velocities. This is illustrated schematically in Fig. 1.

The local macroscopic properties such as total mass (the particle mass, m, is assumed unitary), $\rho(\mathbf{x}, t)$, and total momentum, $\rho\mathbf{u}(\mathbf{x}, t)$, can be obtained from the distribution function according to,

$$\rho(\mathbf{x}, t) = \sum_i f_i(\mathbf{x}, t)\,, \tag{1}$$

$$\rho\mathbf{u}(\mathbf{x}, t) = \sum_i f_i(\mathbf{x}, t)\mathbf{c}_i\,. \tag{2}$$

The Lattice Boltzmann equation, i.e., the discrete version of the Boltzmann equation is written as,

$$f_i(\mathbf{x} + \delta_t\mathbf{c}_i, t + \delta_t) - f_i(\mathbf{x}, t) = \Omega_i(\rho, \mathbf{u})\,, \tag{3}$$

where δ_t is the time step and $\Omega_i(\rho, \mathbf{u})$ is the collision operator.

The time evolution given by Eq. (3), can be split in two processes. In the first, designated as collision, the distribution function $f_i(\mathbf{x}, t)$ is changed by the action of the collision operator. In the

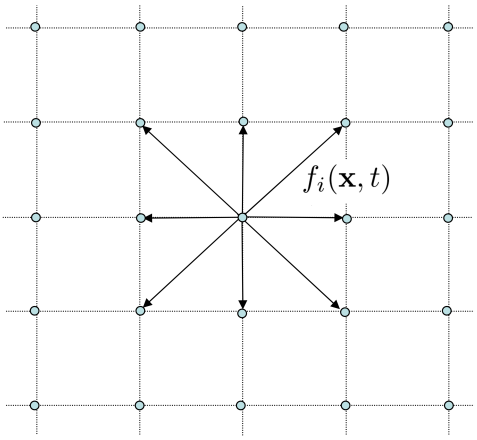

Figure 1. The D2Q9 lattice, used in two-dimensional simulations. The arrows represent the distributions $f_i(\mathbf{x}, t)$, and circles represent the lattice sites.

second process, called propagation, the values f_i are propagated to the neighboring sites, in accordance with the direction of the vector $\mathbf{c}_i$.

Owing to its simplicity, the most widely used collision operator is the BGK operator, written as,

$$\Omega_i = -\frac{1}{\tau/\delta_t}\left[f_i(\mathbf{x}, t) - f_i^{eq}(\rho, \mathbf{u})\right] , \tag{4}$$

where τ is a relaxation parameter related to the kinematic viscosity ν and $f_i^{eq}(\rho, \mathbf{u})$ is a polynomial approximation of the Maxwell-Boltzmann equilibrium distribution function of the local variables $\rho(\mathbf{x}, t)$ and $\mathbf{u}(\mathbf{x}, t)$ [20–23]. Another frequently used collision operator for simulation in porous media is TRT collision operator [19]. In this collision operator the distribution function is separated into its symmetric (+) and anti-symmetric (-) components:

$$f_i^{\pm} = \frac{1}{2}(f_i \pm f_{-i}), \qquad i = 1, ..., b; \tag{5}$$

where the label $-i$ indicates the opposite direction of $\mathbf{c}_i$, that is $\mathbf{c}_{-i} = -\mathbf{c}_i$. For the rest populations $f_0^+ = f_0$, $f_0^- = 0$. The TRT collision operator is then written,

$$\Omega_i = -\frac{1}{\tau/\delta_t}\left[f_i^+(\mathbf{x}, t) - f_i^{eq+}(\rho, \mathbf{u})\right] - \frac{1}{\tau^-}\left[f_i^-(\mathbf{x}, t) - f_i^{eq-}(\rho, \mathbf{u})\right] , \tag{6}$$

where τ^-, the anti-symmetric relaxation time, is a function of τ,

$$\tau^- = \frac{8 - \delta_t/\tau}{8(2 - \delta_t/\tau)}. \tag{7}$$

The symmetric and anti-symmetric equilibrium distributions are obtained by applying Eq. (5) to the equilibrium distributions.

A Chapman-Enskog analysis [24] shows that this system macroscopically will evolve according to the Navier-Stokes equations,

$$\frac{\partial \rho}{\partial t} + \frac{\partial (\rho u_j)}{\partial x_j} = 0 , \tag{8}$$

$$\frac{\partial (\rho u_k)}{\partial t} + \frac{\partial (\rho u_k u_j)}{\partial x_j} = -\frac{\partial p}{\partial x_k} + \nu \frac{\partial}{\partial x_j}\left(\rho \frac{\partial u_j}{\partial x_k} + \rho \frac{\partial u_k}{\partial x_j}\right) , \tag{9}$$

where the pressure p and the kinematic viscosity ν are given by,

$$p = c_s^2 \rho , \tag{10}$$

$$\nu = c_s^2(\tau - 1/2) . \tag{11}$$

and c_s is the sound velocity, a constant depending on the set of velocities $\mathbf{c}_i$. In the simulations presented in this paper a set with nine velocities is employed, shown in Figure 1.

2.2 Simulation Domain

The simulation domain shown in Figure 2 was discretized at the finest resolution using 150 sites uniformly distributed in the wall normal direction over the span H, $N_H = 150$. This spatial resolution was maintained over the entire simulation domain. In our previous work, we established that a conservative length $l_d = 100h$ was sufficient to ensure that domain size effects over the flow of the backward facing step are negligible. In all of our simulations, $l_d = 10h$. Barkley et al. [25] have also shown this to be the case.

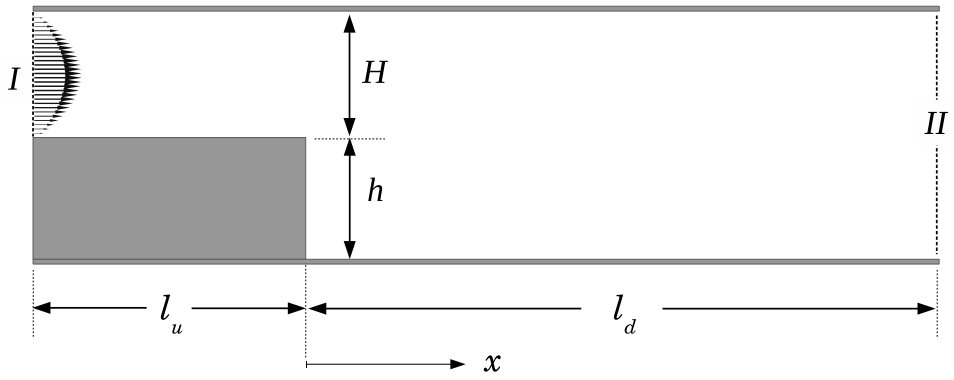

Figure 2. The D2Q9 lattice, used in two-dimensional simulations. The arrows represent the distributions $f_i(\mathbf{x}, t)$, and circles represent the lattice sites.

2.3 Boundary and Initial Conditions

At the walls the bounce-back boundary conditions for particle distributions were imposed, i.e., all particles that would collide with the walls in the propagation step reverse their direction in this step. This ensures the no-slip boundary condition at the walls and was chosen owing to its simplicity. At the inlet (I) a parabolic laminar velocity profile was imposed using the Zou & He boundary condition, [26]. At the outlet (II) of the domain a null-derivative boundary condition in the direction of the flow was applied. This is obtained by imposing that sites at the outlet assume the velocity of the adjacent sites. All sites are initialized with zero velocity by imposing the equilibrium distribution. The flow develops as a result of the boundary condition imposed at the inlet. Only after the elapsed simulation time is $t \sim \mathcal{O}(100)$ of the time scale H/U, statistics begin to be computed.

The incompressible solver icoFoam available in OpenFOAM was used to corroborate LBM simulations. The same parabolic inlet velocity was prescribed along with a pressure gradient boundary condition to ensure that the flux at the inlet boundary is that specified by the velocity boundary condition. The outflow boundary condition for pressure was set to 0 and the velocity outflow boundary condition was set to a null streamwise derivative. The same spatial resolution as the LBM solvers was adopted. The time step was set to ensure a Courant number of less than 0.35 during almost the entire simulation, excluding a brief initial period. At no moment did the Courant number exceed unity.

3 Results and Discussion

In this section we present the results obtained in simulations using LBM with BGK and TRT operators. The results are compared with each other and with results obtained from OpenFOAM as well as experimental and numerical results previously reported in Tihon et al. [17]. The variable of choice for

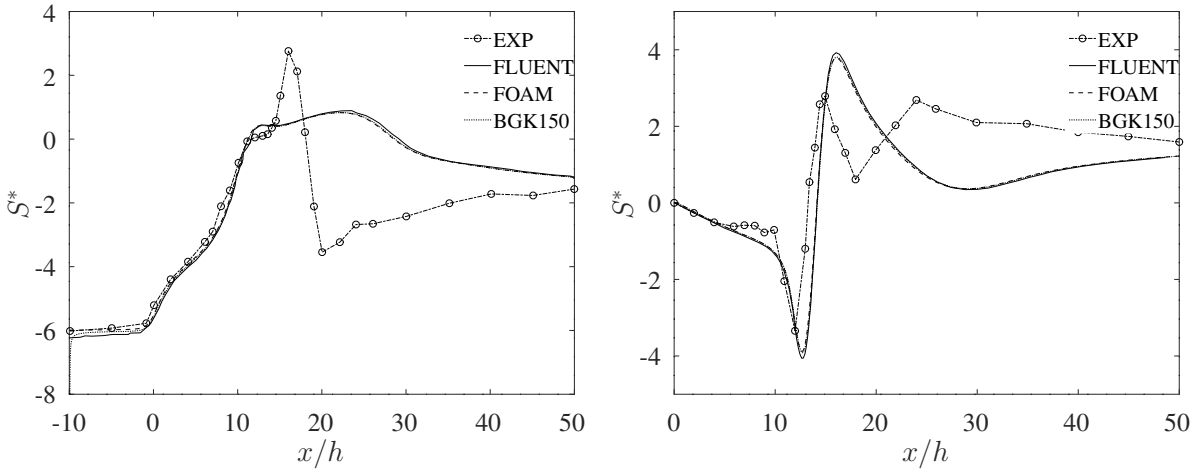

(a) (b)

Figure 3. BGK comparison of the non-dimensional mean shear rate S^* at the (a) top and (b) bottom channel wall with previous results of Tihon et al. [17] (EXP, FLUENT) and OpenFoam (FOAM).

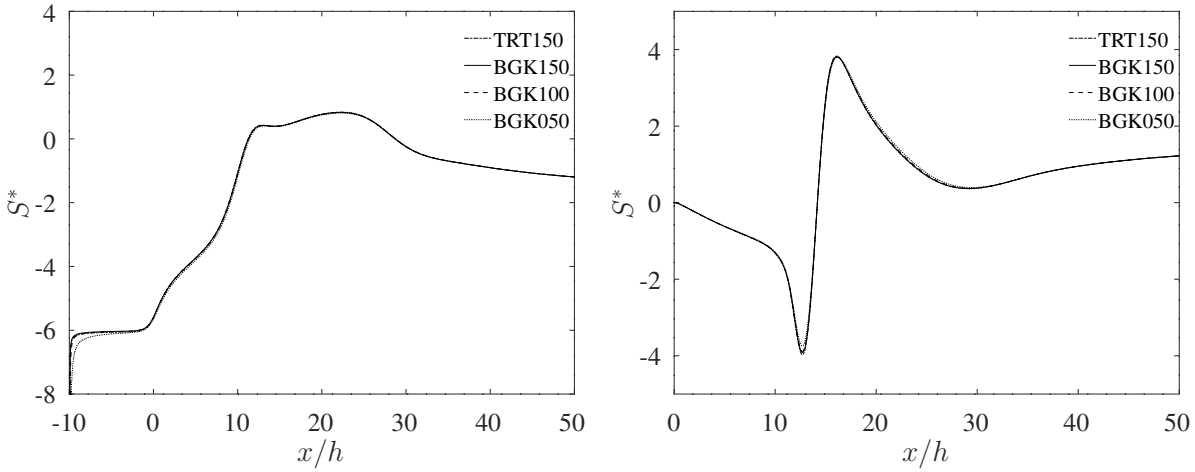

(a) (b)

Figure 4. Comparison of the non-dimensional mean shear rate S^* at the (a) top and (b) bottom channel wall among TRT and BGK collision operator implementations of the LBM.

comparison is the non-dimensional mean shear rate at the top and bottom wall S^*, given by,

$$S^* \equiv \frac{h}{U}\frac{\partial u}{\partial y}\bigg|_{\text{wall}} \approx \frac{1}{2}\frac{h}{U}\frac{u_{\text{near}}}{\delta_n}, \tag{12}$$

where δ_n is the grid spacing in the wall-normal direction and u_{near} is the velocity component in the streamwise direction at the grid node closest to the wall.

The shear rate is calculated after the system reaches steady state. This is quantified in terms of an integral timescale defined as $\tau_h = h/U$. After this steady state is reached $\mathcal{O}(10^2\tau_h)$ the average shear rate calculated over a period of $\mathcal{O}(10\tau_h)$.

As can be seen in Figures 3 and 4, the results obtained with both operators are in very close agreement with respect to each other and with results obtained using OpenFoam as well as published numerical

results by Tihon et al. [17]. The numerical results shown here are in reasonable agreement with experimental results of of Tihon et al. [17] up to $x/h = 15$. As shown in the work of Barkley et al. [25], the first absolute linear instability of the steady two-dimensional flow is a steady three-dimensional bifurcation at a critical Reynolds number of $Re_h = 748$. Furthermore, the system is shown to be absolutely stable to two-dimensional perturbations up to a Reynolds number of $Re_h = 1500$. Hence, the discrepancies shown are not likely to be related to 3-D effects since both 2D-simulations and experiments are not expected to show three-dimensional features at the Reynolds number of $Re_h = 590$. Our simulations from a quiescent initial condition reveal features very similar to the experimental results shown in Figures 3.

With respect to the comparison of collision operators, BGK proved to be considerably more stable than TRT. Furthermore, the smallest spatial resolution at which TRT was stable was with $N_H = 150$, whereas with the BGK operator it was possible to obtain similar results with $N_H = 50$. The reasons for the instability of the TRT operator are still unclear at the time of writing of this paper and shall be the subject of future investigation.

4 Conclusions

In this paper we present results for the 2-D simulation of a flow over a backward-facing step at $Re_h = 590$. We investigate the numerical stability of the TRT and BGK operators with respect to spatial resolution. It is found that the BGK operator is significantly more stable than the TRT operator for this flow. LBM simulation results compare favorably with a simulation using OpenFOAM and previous results reported in the literature. Future work will address the issue of numerical stability of the LBM implementation with the TRT collision operator.

References

[1] Eaton, J. K. & Johnston, J. P., 1981. A review of research on subsonic turbulent flow reattachment. *AIAA Journal*, vol. 19, n. 9, pp. 1093–1100.

[2] Theofilis, V., 2011. Global linear instability. *Annual Review of Fluid Mechanics*, vol. 43, pp. 319–352.

[3] Abe, K. & Kondoh, T., 1994. A new turbulence model for predicting fluid flow and heat transfer in separating and reattaching flows—i. flow field calculations. *International Journal of Heat and Mass Transfer*, vol. 37, pp. 139–151.

[4] Cabot, W., 1996. Near-wall models in large-eddy simulations of flow behind a backward-facing step. In *Annual Research Briefs*, pp. 199–210. Center for Turbulence Research.

[5] Piomelli, U. & Balaras, E., 2002. Wall layer models for large-eddy simulations. *Annual Review of Fluid Mechanics*, vol. 34, pp. 349–374.

[6] Armaly, B. F., Durst, F., Pereira, J. C. F., & Schönung, B., 1983. Experimental and theoretical investigation of backward-facing step flow. *Journal of Fluid Mechanics*, vol. 127, n. -1, pp. 473.

[7] Kasagi, N. & Matsunaga, A., 1995. Three-dimensional particle-tracking velocimetry measurement of turbulence statistics and energy budget in a backward-facing step flow. *International Journal of Heat and Fluid Flow*, vol. 16, pp. 477–485.

[8] Kostas, J., Soria, J., & Chong, M., 2002. Particle image velocimetry measurements of a backward-facing step flow. *Experiments in Fluids*, vol. 33, pp. 838–853.

[9] Piirto, M., Saarenrinne, P., Eloranta, H., & Karvinen, R., 2003. Measuring turbulence energy with piv in a backward-facing step flow. *Experiments in Fluids*, vol. 35, pp. 219–236.

[10] Lee, T. & Mateescu, D., 1998. Experimental and numerical investigation of 2-D backward-facing step flow. *Journal of Fluids and Structures*, vol. 12, pp. 703–716.

[11] Malamataris, N. A., 2013. A numerical investigation of wall effects in three-dimensional, laminar flow over a backward facing step with a constant aspect and expansion ratio. *International Journal for Numerical Methods in Fluids*, vol. 71, n. 9, pp. 1073–1102.

[12] LE, H., MOIN, P., & KIM, J., 1997. Direct numerical simulation of turbulent flow over a backward-facing step. *Journal of Fluid Mechanics*, vol. 330, n. 8, pp. 349–374.

[13] Barri, M., El Khoury, G. K., Andersson, H. I., & Pettersen, B., 2010. Dns of backward-facing step flow with fully turbulent inflow. *International Journal of Numerical Methods in Fluids*, vol. 64, pp. 777–792.

[14] Succi, S., 2001. *The Lattice Boltzmann Equation for Fluid Dynamics and Beyond*. Oxford University Press.

[15] Aidun, C. K. & Clausen, J. R., 2009. Lattice-Boltzmann method for complex flows. *Annual Review of Fluid Mechanics*, vol. 42, pp. 439–472.

[16] Salazar, J. P. d. L. & dos Santos, L. O. E., 2014. 2D LATTICE-BOLTZMANN SIMULATIONS OF FLOW OVER A BACKWARD-FACING STEP AT LOW TO MODERATE REYNOLDS NUMBERS. *Cilamce2014 XXXV Iberian Latin American Congress on Computational Methods in Engineering*.

[17] Tihon, J., Pěnkavová, V., & Pantzali, M., 2010. The effect of inlet pulsations on the backward-facing step flow. *European Journal of Mechanics, B/Fluids*, vol. 29, n. 3, pp. 224–235.

[18] Qian, Y. H., D'Humières, D., & Lallemand, P., 1992. Lattice BGK Models for Navier-Stokes Equation. *Europhysics Letters*, vol. 17, pp. 479–484.

[19] Ginzburg, I. & D'Humières, D., 2003. Multireflection boundary conditions for lattice Boltzmann models. *Physical Review E - Statistical Physics, Plasmas, Fluids, and Related Interdisciplinary Topics*, vol. 68, n. 6, pp. 1–30.

[20] Abe, T., 1997. Derivation of the lattice Boltzmann method by means of the discrete ordinate method for the Boltzmann equation. *Journal of Computational Physics*, vol. 131, n. 1, pp. 241–246.

[21] He, X. Y. & Luo, L. S., 1997. A priori derivation of the lattice Boltzmann equation. *Physical Review E*, vol. 55, n. 6, pp. R6333–R6336.

[22] Shan, X., Yuan, X.-F., & Chen, H., 2006. Kinetic theory representation of hydrodynamics: a way beyond Navier-Stokes equation. *Journal of Fluid Mechanics*, vol. 550, pp. 413–441.

[23] Philippi, P. C., Hegele, L. A., dos Santos, L. O. E., & Surmas, R., 2006. From the continuous to the lattice Boltzmann equation: The discretization problem and thermal models. *Physical Review E*, vol. 73, n. 5, pp. 56702.

[24] Chapman, S. & Cowling, T. G., 1970. *The theory of non-uniform gases*. Cambridge University Press, 3 edition.

[25] Barkley, D., Gomes, M. G. M., & Henderson, R. D., 2002. Three-dimensional instability in flow over a backward-facing step. *Journal of Fluid Mechanics*, vol. 473, pp. 167–190.

[26] Zou, Q. & He, X., 1997. On pressure and velocity boundary conditions for the lattice Boltzmann BGK model. *Physics of Fluids*, vol. 9, n. 1591.